

IMPURITY BEHAVIOUR FOR VARIOUS AUXILIARY HEATING METHODS IN ASDEX

G. Fussmann, R. Bartiromo¹, G. Janeschitz, P.B. Kotzé², E. R. Müller, F. Söldner, H. S. Bosch, A. Eberhagen, O. Gehre, J. Gernhardt, G. v. Gierke, E. Glock, O. Gruber, G. Haas, F. Karger, M. Keilhacker, A. Kislyakov³, O. Klüber, M. Kornherr, M. Lenoci¹, G. Lisitano, A. Mahdavi⁴, H.-M. Mayer, K. McCormick, D. Meisel, V. Mertens, H. Murmann, H. Niedermeyer, W. Poschenrieder, H. Rapp, F. Ryter⁵, J. Roth, F. Schneider, G. Siller, P. Smeulders, E. Speth, K. Steinmetz, K.-H. Steuer, O. Vollmer, F. Wagner and F. Wesner

Max-Planck-Institut für Plasmaphysik
EURATOM Association, D-8046 Garching

Introduction: Three different additional heating methods are being applied in the ASDEX divertor tokamak: neutral injection (NI), ion cyclotron heating (ICRH) at the 2nd harmonic of hydrogen, and lower hybrid heating (LH). In this paper we discuss the impurity behaviour observed for three heating scenarios. Applying all three methods in the same tokamak has the advantage of allowing a fair comparison of the concomitant impurity problems. Such a phenomenological comparison of the impurity levels has been made for the most important elements Fe, Ti, O, and C. A more profound judgement of the impurity problem, however, will have to distinguish between impurity production, penetration depth of the neutrals into the plasma boundary, and transport in the scrape-off and inner plasma regions. We are not yet in a position to identify the actual importance of these different causes, but some preliminary information was obtained from our measurements. Furthermore, the identification of the dominant production mechanisms is also a matter of crucial importance. We briefly address the problem of sputtering of wall material (Fe) by CX neutrals during NI and access the evidence for the prelinance of ion sputtering in the case of both HF-heating methods.

NI heating: Neutral injection has been applied in ASDEX up to a power level of 4.2 MW ($\Delta t \leq 0.4$ s, D^0 or H^0 with $E \leq 45$ keV). The impurity problems arising with this additional heating are in general tolerable ($P_{\text{rad}}/P_{\text{tot}} \leq 20\%$) with the exception of the cases where the quiescent H-mode had been realized. In this latter case a radiation collapse is observed ($P_{\text{rad}} \sim 3$ MW) which can be attributed to accumulation of iron $/1/$. Typical concentrations for the ohmic phase and the normal H-phase of NI ($P_{\text{NI}} = 2.8$ MW, $\bar{n}_e = 2.5 \times 10^{13}$ cm⁻³, D_2) are in the range: O: 0.15 % (OH), 0.6 - 1 % (NI); Fe: 0.2×10^{-4} (OH), 1.2×10^{-4} (NI). Simulating the impurity behaviour with a time dependent transport code - using measured T_e and n_e profiles as input data - yield some information on the transport parameters and the impurity fluxes. For D_2 discharges we find $D \sim 4000$ cm²/s for OH and the normal H-phase, and $D \sim 10^4$ cm²/s for the L-phase of NI. In addition, a moderate inward drift velocity of $v_{\text{in}} = -2D r/a^2$ is indicated. The Fe fluxes increase for the above NI power level by a factor of 20 to $\Gamma_{\text{Fe}} = 3 \times 10^{13}$ cm⁻² s⁻¹ with respect to the OH phase. In order to estimate the influence of a change

¹ENEA Frascati, Italy; ²Nuclear Development Corp. of South Africa, Pretoria
³Ioffe Institute, Leningrad, USSR; ⁴GA Technologies, San Diego, USA;
⁵CEN Grenoble, France

in penetration depth with the transition from OH + L + H the measured boundary profiles /2/ of n_e and T_e were properly taken into account in the transport calculations. For unchanged Fe fluxes we should thus expect a change of concentrations according to 1 (OH) + 0.3 (L) + 0.8 (H) for the three phases. It should be noted, however, that these ratios are actually tendency factors because of the sensitivity with regard to the exact position of the separatrix and the absolute values of T_e . The rather low screening efficiency during the H-phase results in particular from the low T_e and n_e values in the scrape-off.

To address the question of Fe production, discharges were performed in H₂, D₂, and He. An extended discussion of the ohmic phase of these experiments is given in /2/. The behaviour of two Fe line intensities as well as soft X ray and bolometer traces for the NI phase are depicted in Fig. 1 for the three different gas fillings ($P_{NI} = 2.8$ MW, L-phase, H⁰, E = 45 keV). For similar densities ($n_{e0} = 3.5, 3.3, 3.8 \times 10^{13} \text{ cm}^{-3}$) the temperatures measured were $T_{e0} = 1.25, 1.80, 1.55$ keV in the case of H⁺, D⁺, He⁺⁺ background ions, respectively. The iron concentrations $n_{Fe}(0)/n_e(0)$ in the corresponding cases were found to be $1.1 \times 10^{-4}, 1.0 \times 10^{-4}$, and 2.4×10^{-4} . In particular, the high concentrations in the case of He are surprising in view of the low He⁺⁺-He⁰ CX cross-sections and the impossibility of producing high-energy neutrals in the core plasma via charge exchange with H⁺ beam particles. Whether sufficient CX neutrals are still produced in the outer plasma regions - as is conjectured for the ohmic phase in /3/ - to explain our results needs further investigation.

ICRH heating: First attempts with ICRH revealed serious impurity problems. In comparison with NI much higher Fe concentrations were found even for lower heating powers. An example is shown in Fig. 2 where during the same discharge 900 kW of NI and 450 kW of ICRH power were launched into the torus. We ascertain a strong increase of the Fe intensities and a further rise of the main plasma radiation losses (bolometer) with ICRH, whereas the C III signals in the main chamber and in particular in the divertor are found to decrease. This decrease of the divertor radiation is indicative of reduced power flow into the divertor, consistent with the enhanced radiation losses from the main plasma ($P_{rad}/P_{tot} = 20\% \rightarrow 40\%$). A considerable improvement - reduction of the power losses by up to a factor of 2 - was achieved by operating at toroidal field strengths where the ion cyclotron resonance layer coincides with the divertor entrance /3/: This observation suggests that the enhancement of the Fe fluxes is caused by up drifting suprathermal ions being produced in the resonance zone. In any case, an additional Fe production mechanism probably has to be postulated since the impurity levels are already substantially increased for marginal changes of CX-fluxes and ion temperatures.

The best heating results are obtained by combining ICRH with NI. There may be two reasons for the beneficial effect of NI: better coupling of the wave to the plasma due to pre-heating, and in addition thermal stabilization of the scrape-off, this being required to prevent deep penetration of the impurities owing to a decrease of temperature in this region. However, also with NI and under optimized ICRH conditions an overproportional increase of the radiation losses with the onset of ICRH is found. In Fig. 3 this behaviour is documented for three different power levels $P_{ICRH} = 0.6, 1.8$, and 2.45 MW, overlapping with NI heating at 1.75 MW. Adding the same power of 1.8 MW to NI is seen to increase the soft X-ray ($h\nu > 400 \text{ eV}$) and Fe XVI intensities by a factor of 5 to 6. According to our transport code analysis this increase directly reflects the enhancement of the Fe fluxes since the T_e and n_e profile changes are small ($T_{e0} = 1.34 \rightarrow 1.57 \text{ keV}$) and the trans-

port parameters can be assumed to be effectively determined by NI heating (L-phase). Further confirmation of these assumptions is inferred from the OVIII signals shown in Fig. 3, which exhibit only a moderate and non-monotonic increase with ICRH power. For the cited case of $P_{NI} = P_{ICRH} = 1.8$ MW we obtain $n_{Fe}(0) = 3.1 \times 10^{10} \text{ cm}^{-3}$ ($n_{Fe}(0)/n_e(0) = 7 \times 10^{-4}$) and a total flux of $\Phi_{Fe} = \Gamma_{Fe} \times 2.5 \times 10^{19} \text{ cm}^{-2} = 2.4 \times 10^{19} \text{ s}^{-1}$. This flux is to be compared with the stationary H^+ flux leaving the plasma, which, however, is not well known in the case of additional heating. Taking for reference the ohmic recycling flux $\Phi(H^+) \sim 2 \times 10^{21} \text{ s}^{-1}$ as a lower limit /4/ and multiplying it by the maximum sputtering rate of 1% (H^0 on SS), we obtain just the above Fe flux. Despite the rather large uncertainties, these considerations suggest that the outdrifting suprathermals are an appreciable fraction of the total ion flux.

LH heating: Apart from initial difficulties, caused by arcing at the grill antenna and neighbouring surfaces, no serious impurity problems generally occur with LH-heating. This statement, however, should be qualified by adding that so far only moderate powers (≤ 0.7 MW) could be launched into the torus /5/. The impurity behaviour in the case of LH shows a pronounced trend with density. In Fig. 4 a comparison between ohmic and LH heated plasmas ($P_{LH} = 400 \text{ kW}$, D_2 , $I_p = 300 \text{ kA}$, $B_0 = 2.17 \text{ T}$, $\bar{n}_n = 4$, mode: $\pi 0 \pi 0 \pi$) is shown. Plotted in the figure are the increment of the radiation loss and the ratios of the Fe XVI, CIII and OVI line intensities as functions of \bar{n}_e . For $\bar{n}_e \leq 2 \times 10^{13} \text{ cm}^{-3}$ the waves are coupled preferentially to suprathermal electrons. In this regime efficient plasma heating is found and the increase of radiation losses is small /5/. For higher densities coupling to the ions becomes predominant /6/. For this regime the production of badly confined suprathermal ions in the boundary region with characteristic tail energies of 3-4 keV was substantiated by CX diagnostics /7/. The corresponding fluxes increase with density up to $\bar{n}_e = 4.5 \times 10^{13} \text{ cm}^{-3}$. It can be assumed that these particles cause the steep increase of iron above $\bar{n}_e = 2 \times 10^{13} \text{ cm}^{-3}$, as shown in Fig. 4.

Summary: Impurity problems arising with auxiliary heating are mainly caused by metallic impurities (Fe and to some extent Ti and Cr being released from the wall of the plasma chamber. These impurities result in peaked radiation profiles (bolometer profile measurements) with non-negligible power losses in the plasma centre. The worst case is observed for the quiescent H-mode of NI, where improved confinement leads to impurity accumulation. Apart from this exceptional case, the impurity concentrations found during NI are comparatively low. In respect of our He experiments, however, the Fe production mechanisms during NI are still uncertain. There are several indications that the increase of Fe concentration in the case of ICRH and LH can be attributed to enhanced Fe production caused by suprathermal ion sputtering. When the three heating methods are compared, ICRH is found to produce the highest Fe densities for the same power input. However, in this case too, the total power losses can be kept tolerable ($\leq 35\%$) when combining ICRH with NI.

References

- /1/ M. Keilhacker et al., Proc. 10th Int. Conf. on Plasma Physics and Contr. Nucl. Fus. Research, London (1984), IAEA-CN-44/A II-1
- /2/ J. Roth et al., this conference
- /3/ K. Steinmetz et al., this conference
- /4/ G. Haas et al., J. Nuclear Materials 121 (1984), 151-156
- /5/ F. Söldner et al., this conference
- /6/ F. Leuterer et al., Proc. 10th Int. Conf. on Plasma Physics and Contr. Nucl. Fus. Research, London (1984), IAEA-CN-44/F-IV-3
- /7/ D. Eckhardt et al., 4th Int. Symp. on Heating in Toroidal Plasmas, Rome (1984)

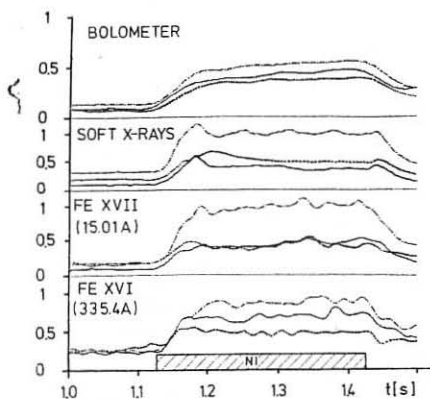


Fig. 1: Traces of bolometer, soft X-ray, and Fe line intensities during ohmic and NI phase (2.8 MW) for various filling gases: H_2 (solid), D_2 (dotted), and He (dashed-dotted).

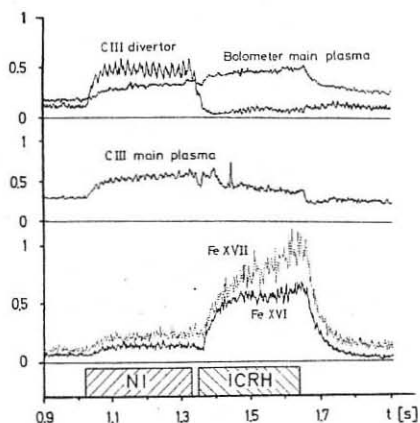


Fig. 2: Comparison between NI (900 kW) and ICRH (450 kW) heated plasmas. Plotted vs. time are radiation losses (bolometer), CIII and Fe line intensities from main plasma, and a CIII divertor signal.

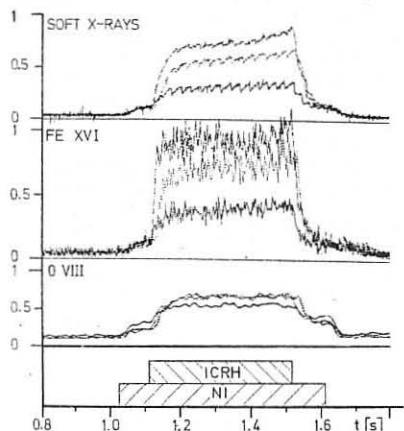


Fig. 3: Soft X-rays, Fe XVI (335 Å) and O VIII (19 Å) line intensities for combined NI (1.75 MW) and ICRH heating: $P_{ICRH} = 0.6$ (solid lines), 1.8 (dotted), and 2.45 MW (dashed-dotted).

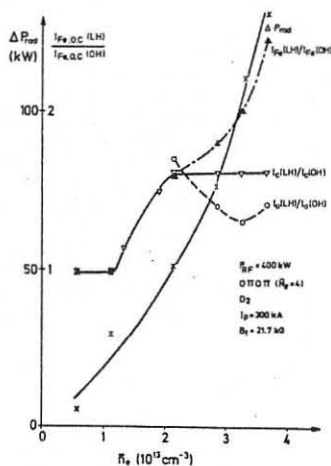


Fig. 4: Increase of radiation losses ΔP_{rad} vs. density for LH heating. Also shown are intensity ratios with respect to ohmic heating for Fe XVI, OVI and CIII emission.